

Growth of AOT Reversed Micelles and the Solvent Effect Investigated by Dielectric and Light-Scattering Measurements

Reiji Tanaka,* Takuya Yokoyama, Kaori Sameshima, and Tokuzo Kawase¹

Department of Chemistry, Graduate School of Science, Osaka City University,
Sugimoto, Sumiyoshi-ku, Osaka 558-8585

¹Department of Chemistry and Materials Technology, Kyoto Institute of Technology, Kyoto 606-8585

Received August 27, 2004; E-mail: rtanaka@sci.osaka-cu.ac.jp

The relative permittivity (ϵ_r) and the conductivity (κ) at a frequency (f) of 50 kHz, and the dynamic light-scattering were measured for ternary systems of (AOT + r ·H₂O) solved in cyclohexane, heptane, octane, decane, and dodecane at a temperature of 298.15 K as a function of the amount ratio (r) of water to AOT ($r = [\text{H}_2\text{O}]/[\text{AOT}]$) up to the onset of percolation. The molality (m) of AOT for those solutions was 0.15 mol kg⁻¹, and increased to 0.30 mol kg⁻¹ for solutions with dodecane. By increasing r , spherical reversed micelles were formed at $r \approx 6$ in straight-chain hydrocarbons. The light-scattering measurements indicated that the mean hydrodynamic diameter of the micelles increased with increasing r , showing a sigmoid curve. The growth of micelles was promoted in a longer chain hydrocarbon. The percolation transition occurred as the particles grew to a critical diameter of about 50 nm. On the other hand, the growth of particles in *c*-hexane was moderate, and percolation did not occur up to $r = 90$, where the solution turned turbid. The growth of particles found from light-scattering measurements was well correlated to dielectric observations.

Ternary mixtures composed of AOT (sodium bis(2-ethylhexyl) sulfosuccinate), water, and oil have attracted much interest, since they form a thermodynamically stable phase, called a microemulsion. The percolation transition, which causes a steep rise in the conductance as the temperature is increased, is one of the most-studied phenomena for this system.^{1–6} Concerning the mechanism of the conductance increment at the vicinity of the percolation threshold, a “hopping” of the AOT anion was investigated in earlier studies.^{7–11} Another model addresses the transfer of counter ions through water channels opening in clusters.^{12–14} Recently, an alternative dynamic-model has been proposed, which assumes the exchange of Na⁺ due the fusion–fission process taking place between two droplets, rather than “hopping” of the AOT anion. This process occurs at a lower temperature of percolation onset; above the transition temperature, static water-channels are formed among reversed micelles.¹⁵ The dynamic transfer of Na⁺ was ascertained by forming the bridging of a pair droplets, brought about by such additives as aromatic hydrotropes.¹⁶ It is well known that the hydrocarbon length used for the solvent is responsible for percolation onset. Previously, we determined the relative permittivity (ϵ_r) and the electric conductivity (κ) for systems of (AOT + r ·H₂O + alkane) as a function of r at a temperature (T) of 298.15 K.¹⁷ We concluded that the linear chain hydrocarbons penetrates the outer shell of reversed micelles, and make the hydrophobic shell rigid. Accordingly, a small curvature of the outer shell is favored, resulting in the formation of a larger size of micelles in a solvent of longer chain hydrocarbons. Penetration of the solvent hydrocarbon into the outer shell of microemulsion droplets has also been suggested by some authors. Gruen and his co-worker described that a short-chain alkane, such as hexane,

strongly penetrates, but a long-chain alkane, such as hexadecane, does not absorb into the surfactant tail region.^{18,19} Although it is considered that the attractive interaction between the microemulsion droplets increases as the chain length of the solvent alkane increases,^{5,20} the mechanism of the solvent effect has not been well analyzed.

The percolation transition also occurs when r is increased to a binary solution of (AOT + hydrocarbon) at a constant temperature. Along with this process we can pursue the formulation and growth of an AOT assembly occurring with the help of water from the view point of molecular interactions. As a powerful tool to determine the structure of the microemulsion, small-angle neutron scattering^{21–23} and small-angle X-ray scattering are used.^{24,25} However, those methods are not easy to use. A more convenient one is a light-scattering measurement, although it is only useful for clear and relatively dilute solutions. In order to confirm the correlation between the observed dielectric behavior and the growth of assemblies of reversed micelles, we carried out a light-scattering measurements for mixtures of {(AOT + r ·H₂O) + *c*-hexane, + heptane, + octane, + decane, and + dodecane} as a function of r at $T = 298$ K. Since the properties and structure of a W/O microemulsion change sensitively with the experimental conditions, such as T , m , r , salinity, and solvent, systematic and precise measurements are required. Because measurements of light-scattering were carried out at $m = 0.15$ mol kg⁻¹, the dielectric properties were measured at the same molality to make a comparison.

Experimental

Materials. The purification of AOT (Aldrich Chemical Co., purity > 98%) to remove salts was similar to that in a previous

process.¹⁷ According to the Karl Fischer's method, the mole fraction of water in AOT was 0.02. Cyclohexane, heptane, and octane were special-grade materials of Wako Pure Chemical Industries, Ltd., and were purified with a 100 cm height distillation column. Decane and dodecane were Cica-reagent materials of Kanto Chemical Co., Inc. Decane was used as received. Dodecane was purified under reduced pressure. The purity of each hydrocarbon was better than 99.95 mole fraction according to glc analysis. Water was purified by using an osmosis membrane (Millipore Co., Milli-Q Labo).

Dielectric Measurements. Measurements of the electrical capacitance (C) and conductance (G) were carried out with a LCR meter (Hewlett-Packard; model HP-4284A) at $f = 50$ kHz and $T = 298.15$ K. A stepwise dilution method was applied to measure the dielectric properties. The basic construction of the electrode cell was similar to the previous one,¹⁷ but its volume was reduced to 40 cm³ from 180 cm³ of the previous one. It consisted of two cylindrical nickel plates, 6 cm in height and 32 mm in diameter for the inner cylinder, with a 3 mm clearance between the two plates. The capacitance of the cell in vacuum was about 28 pF with a lead-capacitance of 4 pF. It was immersed in an oil bath, and its temperature was controlled with an instability of ± 0.002 K. The deviation of C was ± 0.0002 pF and that of G was 0.0003 μ S, respectively.

Light-Scattering Measurements. The particle size in AOT micelle solutions was estimated by means of dynamic light scattering using a NICOMP Model 380 (Particle Sizing System) in which a green diode laser (532 nm) was adopted. Scattered light was detected at a fixed angle of 90 degrees. The hydrodynamic diameter (d) of the particles was calculated from the Einstein-Stokes equation on the basis of the translational diffusion coefficient, assuming a sphere. For analyzing the autocorrelation function of the fluctuating scattered light intensity, we employed a mathematical procedure, referred as inversion of the Laplace transform, and nonlinear least-squares analysis. The temperature around the instrument was kept at 298 K with an instability of 0.1 K. Cell tubes that gave good reproducibility to the blank test were selected.

Results and Discussion

In earlier studies, it was commonly considered that AOT forms reversed micelles in a hydrocarbon without adding water.^{21,26–29} We measured the relative apparent molar enthalpy (L_ϕ) and the apparent molar heat capacity ($C_{p,\phi}$) for a mixed solute of (AOT + $r \cdot \text{H}_2\text{O}$) in *c*-hexane to $m = 1.0$ mol kg^{−1} at 298.15 K.³⁰ The values of L_ϕ were slightly endothermic for a system of $r = 0$. Therefore, we concluded that AOT does not form micelles nor aggregates without the help of water. The exothermic values of L_ϕ were observed for (AOT + $r \cdot \text{H}_2\text{O}$) with $r \geq 1$ as m increased. This results suggested that the hydrated AOT with a small amount of water formed aggregates. While a sharp peak that could be attributed to the formation of reversed micelles was observed in $C_{p,\phi}$ for systems of $r \geq 5$, the value of $C_{p,\phi}$ for systems of $r < 5$ decreased monotonously with increasing m . Therefore, the hydrated AOT with $r < 5$ forms only small-size aggregates. Thus, we may call those small aggregates “pre-micelles”, since they are the elemental components to form reversed micelles.

Figure 1 shows the experimental results for the relative permittivity measured at $m = 0.15$ mol kg^{−1}. The first steep increments in ϵ_r for $r > 1$ observed in straight-chain alkanes are due to the formation of hydrated pre-micelles that have a larger

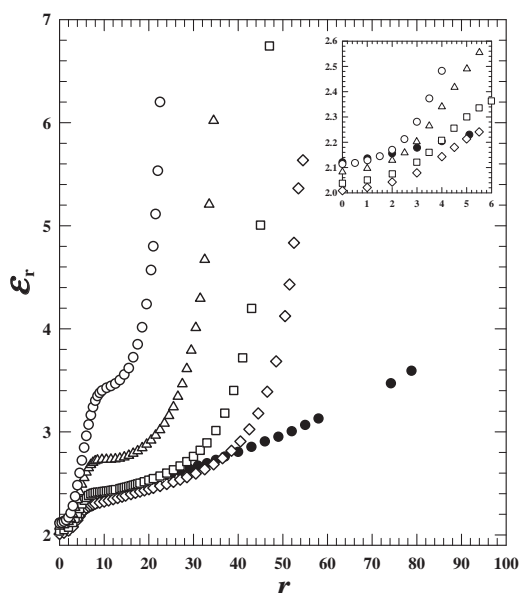


Fig. 1. Relative permittivities (ϵ_r) for (AOT + $r \cdot \text{H}_2\text{O}$ + alkane) measured at $m = 0.15$ mol kg^{−1}, $f = 50$ kHz, and $T = 298.15$ K. ●, *c*-hexane; ◇, heptane; □, octane; △, decane; ○, dodecane.

dipole moment than that of isolated AOT. Therefore, the conformation of the first aggregates formed by the addition of water are asymmetrical. By adding more water, a plateau appeared in the region of $r > 6$ in a straight chain alkane. This implies that the pre-micelles aggregated, while forming spherical assemblies. This was followed by a steep increment because the water in the micelles turned bulky, which had a large permittivity. This increment occurred in parallel with an abrupt increment in the conductivity, as was also found in previous measurements.¹⁷ This is called conductivity percolation. Thus, the steep increment in ϵ_r was due to a percolation onset that accompanied the coalescence of spherical reversed-micelles. The percolation onset shifted to a lower r with increasing length of the solvent alkane. This solvent effect is well known in temperature-induced percolation.³¹ If the straight-chain alkane is accommodated in the hydrocarbon chains of AOT, the outer shell of the micelles will be made rigid due to the dispersion force acting among the hydrocarbons. Accordingly, a smaller curvature is favored, resulting in the formation of large size of particles.¹⁷ Sager and co-workers theoretically analyzed the aggregation process of W/O microemulsion droplets based on the curvature energy concept. They demonstrated that aggregation takes place in the direction of vanishing spontaneous curvature, leading to a structural change from droplets to cylinders, or rod-like aggregates.^{32,33} They carried out small-angle X-ray scattering and proved that a transition occurs from spherical droplets to cylindrical or rodlike aggregates in (AOT + water + 2,2,4-trimethylpentane).²⁴ Their discussions are in agreement with our consideration that straight-chain alkanes penetrate the outer shell of AOT reversed micelles, rather than bridging between the droplets, leading to the formation of a larger size of droplets.

In comparison with the previous results measured at $m = 0.30$ mol kg^{−1},¹⁷ the present magnitude in ϵ_r , measured at $m =$

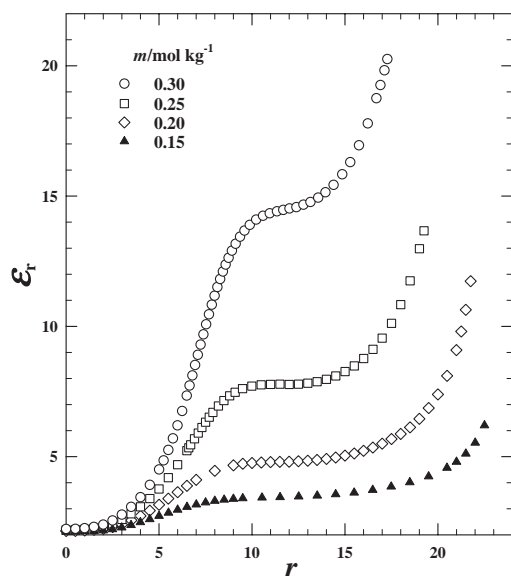


Fig. 2. Relative permittivities (ϵ_r) for (AOT + r ·H₂O + dodecane) measured at $f = 50$ kHz, $T = 298.15$ K, and molalities: \blacktriangle , 0.15 mol kg⁻¹; \diamond , 0.20 mol kg⁻¹; \square , 0.25 mol kg⁻¹; \circ , 0.30 mol kg⁻¹.

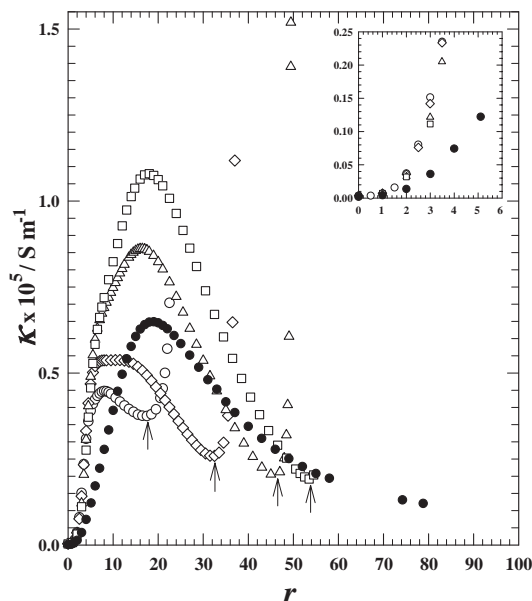


Fig. 3. Conductivities (κ) for (AOT + r ·H₂O + alkane) measured at $m = 0.15$ mol kg⁻¹, $f = 50$ kHz, and $T = 298.15$ K, in solvents: \bullet , *c*-hexane; \square , heptane; \triangle , octane; \diamond , decane; \circ , dodecane.

0.15 mol kg⁻¹, was systematically smaller in each system, and the difference between those two sets became larger along with increasing chain-length of the solvent alkane. Figure 2 shows the permittivities measured in dodecane at various m values up to 0.30 mol kg⁻¹. A plateau appears at nearly the same r regardless of m , while the percolation onset is considerably shifted to a lower r . The increment in ϵ_r beyond the percolation is promoted in a solution of higher m .

Figure 3 shows the experimental results for conductivities

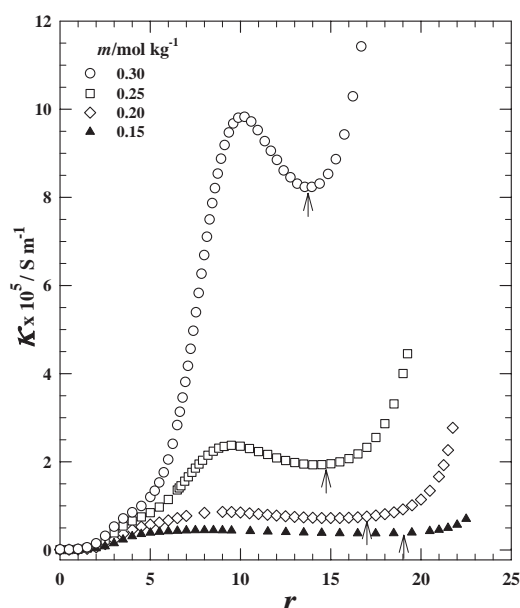


Fig. 4. Conductivities (κ) for (AOT + r ·H₂O + dodecane) measured at $f = 50$ kHz, $T = 298.15$ K, and molalities: \blacktriangle , 0.15 mol kg⁻¹; \diamond , 0.20 mol kg⁻¹; \square , 0.25 mol kg⁻¹; \circ , 0.30 mol kg⁻¹.

measured at $m = 0.15$ mol kg⁻¹. The conductivity begins to increase at $r > 1$. This implies that the aggregation process starts and the created pre-micelles supply the charge carriers. By increasing r , the curve meets a bending, because most charge carriers are trapped in the spherical micelles created by the aggregation of pre-micelles. The percolation onset is indicated by an arrow. It shifts to a lower r with increasing chain length of solvent alkane. In each system, the conductivity shows an abnormal increment, revealing a maximum with increasing r . A typical change was observed in cyclohexane solution.

Figure 4 shows the conductivities measured in dodecane at various m . In each case, the onset of a steep increment is indicated with an arrow. It shifts to a lower r as m increases. An abnormal increment, mentioned above, which is found in the region of $6 < r < 20$, becomes obvious for solutions of $m > 0.20$ mol kg⁻¹, and is quite remarkable in a solution of $m = 0.30$ mol kg⁻¹. A similar change accompanying a shoulder was also reported by Manabe et al. for solutions of (AOT + water + dodecane) measured for $0.05 > m > 0.197$ mol kg⁻¹ at 298 K.³⁴ For this abnormal conductance, a charged-particle model was proposed by Eicke et al.,³⁵ and improved later by Hall.³⁶ An alternative explanation may be given by means of a surface charge model³⁷ that was applied to the dielectric relaxation for (AOT + H₂O + dodecane) by Peyrelasse and Boned.³⁸ However, the mechanism for abnormal conductivity is still open to discussion.

Figure 5 shows the observed results for the hydrodynamic diameter of the AOT assembly as a function of r measured at $m = 0.15$ mol kg⁻¹. In each solvent the diameter at $r = 0$ is about 2.5 nm, and increases with increasing r , showing a sigmoid curve. The light-scattering becomes very unstable beyond the region of percolation onset, especially in short-chain alkanes, since the thermal fluctuation of the particle size is

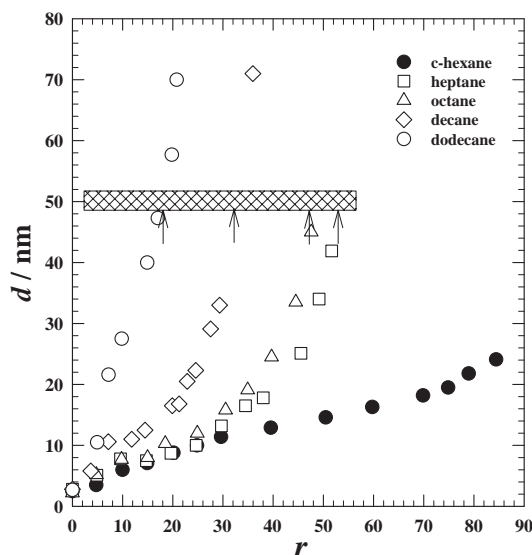


Fig. 5. Hydrodynamic diameters (d) of (AOT + r ·H₂O) particle measured at $m = 0.15$ mol kg⁻¹ and $T = 298$ K in solvents: ●, *c*-hexane; □, heptane; △, octane; ◇, decane; ○, dodecane.

very large. The particle size of AOT reversed micelles varies very sensitively with the experimental condition. Therefore, only few literature values are available to compare with the present results. Wines and Somasundaran reported on the hydrodynamic diameter of AOT reversed micelles with $r = 40$ in heptane at 298 K.³⁹ Their value at $m = 0.15$ mol kg⁻¹ is 21 nm, which agrees very well with ours of 19 nm. According to their report, the particle diameter increases linearly with increasing m , and is consistent with our conclusion obtained from permittivity measurements in dodecane solutions. Kawai et al. reported light-scattering data for systems of (AOT + water + *c*-hexane or 2,2,4-trimethylpentane) at $m = 0.1$ mol kg⁻¹ and 298 K.⁴⁰ However, their curves, plotted as a function of r , considerably differ from our results.

The particle in *c*-hexane gradually grows with increasing r up to 90, where the solution turns turbid. In contrast, the diameter in a straight-chain alkane shows a quite different change with r . A typical change that accompanies a clear plateau in the region of $10 < r < 20$ was observed in heptane and octane. This plateau implies that the growth of particles is restrained as r is increased, while the number of particles of a similar size increases. In this region spherical micelles are formed, as was also suggested from permittivity measurements. The region where the growth of particles is restrained was also found in decane and dodecane. Beyond the plateau, the particle size begins to increase steeply. A dramatic effect of the solvent appears after percolation onset, and in a longer-chain alkane larger assemblies are formed as the same amount of water is added to AOT. In this region, the conductivity decreases once, and then increases again, passing through a minimum due to the percolation transition. The arrow shows the minimum in κ , where the percolation transition starts. It is very interesting to note that the percolation onset occurs as the particle size reaches about 50 nm, regardless of the chain length of the solvent alkane. The hydrodynamic diameter of droplets of AOT with $r = 40$, observed in heptane at 298 K, increased linearly

with increasing m .³⁹ Present measurements, carried out in dodecane at 298 K, showed that the percolation onset shifted to a lower r when m was increased. Sager and Blokhuis concluded that the aggregation of spherical reversed micelles takes place to form cylindrical or rod-like ones.^{32,33} They deduced a critical diameter of spherical droplets to make coalescence. Those results lead us the conclusion that the percolation transition is brought about by the coalescence of reversed micelles that grow to reach a critical size, and it is promoted by the accommodation of solvent alkanes into the AOT tails. Thus, water channels for charge carriers are created, resulting in an abrupt increment in the conductivity and also in the increment in the permittivity because the net-work formation of hydrogen bonding of water is promoted.

An ab initio calculation was performed to estimate the molecular diameter (d) of AOT by GAUSSIAN 98⁴¹ using the method of RHF⁴² with a basis of 6-31G.⁴³ Figure 6 shows the optimized conformations of an extended form (a) and a bending form (b) of isolated AOT. The energy of the extended form is lower by 40.3 kJ mol⁻¹ than that of bending form. Although those optimized conformations are typical ones, the ab initio calculation suggests that AOT molecules solved in non-polar media exist in an extended form, rather than a bending form, in dilute region. The largest separation between atoms is about 2.01 nm for the extended form, while it is 1.46 nm for the bending form. We may not expect an accurate determination of a particle size less than 5 nm by means of light-scattering. However, the observed d of 2.5 nm implies that the isolated AOT tends to take an extended form, but changes to a bending form in *n*-alkanes as water is added. Svergun et al. reported the results of small-angle X-ray scattering for the particle size of (AOT + H₂O) determined for $r = 25$ to 56 in 2,2,4-trimethylpentane at 288.15 K.²⁴ They found that the particles that had d of 2 nm existed irrespective of r . Although they as-

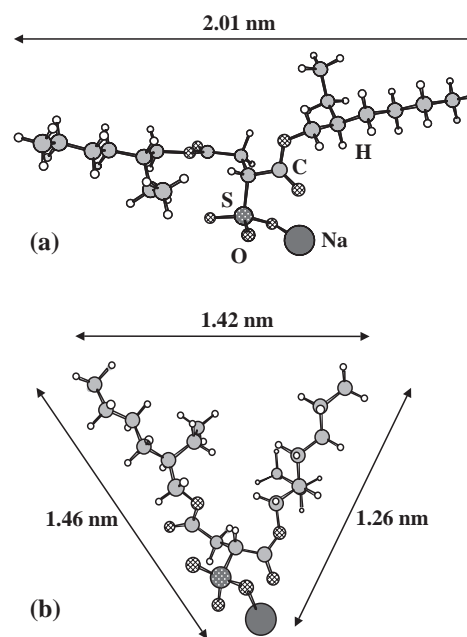


Fig. 6. Optimized conformations of AOT molecule by ab initio calculation. (a), an extended form; (b), a bending form.

signed those particles to AOT reversed micelles, we consider that they were pre-micelles that were in equilibrium with droplets. Eicke and Christen proposed a formation of trimer consisting of $(3\text{AOT} + \text{H}_2\text{O})$.⁴⁴ The dilution enthalpy of a ternary solution of $(\text{AOT} + r \cdot \text{H}_2\text{O} + \text{hydrocarbon})$, solved into the binary solution of $(\text{AOT} + \text{hydrocarbon})$ with the same m , suggested the existence of trimers and pre-micelles.^{45,46}

In the next report we shall turn our attention to the hydration of AOT, and examine the process of forming assemblies by means of calorimetry and theoretical calculations.

References

- S. Bhattacharya, J. P. Stokes, M. W. Kim, and M. J. S. Huang, *Phys. Rev. Lett.*, **55**, 1884 (1985).
- R. Hilfiker, H.-F. Eicke, S. Geiger, and G. Furler, *J. Colloid Interface Sci.*, **105**, 378 (1985).
- A. Jada, J. Lang, and R. Zana, *J. Phys. Chem.*, **93**, 10 (1989).
- H. Mays, J. Pochert, and G. Ilgenfritz, *Langmuir*, **11**, 4354 (1995).
- P. Alexandridis, J. F. Holzwarth, and T. A. Hatton, *J. Phys. Chem.*, **99**, 8222 (1995).
- H. Mays and G. Ilgenfritz, *J. Chem. Soc., Faraday Trans.*, **92**, 3145 (1996).
- M. W. Kim and J. S. Huang, *Phys. Rev. A*, **34**, 719 (1986).
- A. Maitra, C. Mathew, and M. Varshney, *J. Phys. Chem.*, **94**, 5290 (1990).
- G. S. Grest, I. Webman, S. A. Safran, and L. R. Bug, *Phys. Rev. A*, **33**, 2842 (1986).
- A. Ponton, T. K. Bose, and G. Delbos, *J. Chem. Phys.*, **94**, 6879 (1991).
- V. Arcoleo, M. Goffredi, and V. Turco Liveri, *J. Solution Chem.*, **24**, 1135 (1995).
- A. Jada, J. Lang, and R. Zana, *J. Phys. Chem.*, **93**, 10 (1989).
- Y. Feldman, N. Kozlovich, I. Nir, N. Garti, V. Archipov, Z. Idiyatullin, Y. Zuev, and V. Fedotov, *J. Phys. Chem.*, **100**, 3745 (1996).
- H. Mays, *J. Phys. Chem. B*, **101**, 10271 (1997).
- H. Kataoka, T. Eguchi, H. Masui, K. Miyakubo, H. Nakayama, and N. Nakamura, *J. Phys. Chem. B*, **107**, 12542 (2003).
- S. K. Hait, A. Sanyal, and S. P. Moulik, *J. Phys. Chem. B*, **106**, 12642 (2002).
- R. Tanaka and T. Shiromizu, *Langmuir*, **17**, 7995 (2001).
- D. W. R. Gruen and D. A. Haydon, *Pure Appl. Chem.*, **52**, 1229 (1980).
- D. W. R. Gruen, *Chem. Phys. Lipids*, **30**, 105 (1982).
- M. J. Hou, M. Kim, and D. O. Shah, *J. Colloid Interface Sci.*, **123**, 398 (1988).
- S.-H. Chen, *Annu. Rev. Phys. Chem.*, **37**, 351 (1986).
- S.-H. Chen, S.-L. Chang, and R. Strey, *J. Chem. Phys.*, **93**, 1907 (1990).
- M. Nagao, H. Seto, M. Shibayama, and N. L. Yamada, *J. Appl. Crystallogr.*, **36**, 602 (2003).
- D. I. Svergun, P. V. Konarev, V. V. Volkov, M. H. Koch, W. F. C. Sager, J. Smeets, and E. M. Blokhuis, *J. Chem. Phys.*, **113**, 1651 (2000).
- H. Seto, M. Nagao, Y. Kawabata, and T. Takeda, *J. Chem. Phys.*, **115**, 9496 (2001).
- S. Muto and K. Meguro, *Bull. Chem. Soc. Jpn.*, **46**, 1316 (1973).
- K. Kon-no and A. Kitahara, *J. Colloid Interface Sci.*, **35**, 636 (1971).
- A. Kitahara, T. Kobayashi, and T. Tachibana, *J. Phys. Chem.*, **66**, 363 (1962).
- S. G. Frank and G. Zografi, *J. Pharm. Sci.*, **58**, 993 (1969).
- R. Tanaka and M. Adachi, *Netsu Sokutei*, **18**, 138 (1991).
- T. Wolff and H. Hegewald, *Colloids and Surfaces A: Physicochem. Eng. Aspects*, **164**, 279 (2000).
- W. F. C. Sager and E. M. Blokhuis, *Prog. Colloid Polym. Sci.*, **110**, 258 (1998).
- E. M. Blokhuis and W. F. C. Sager, *J. Chem. Phys.*, **110**, 3148 (1999).
- M. Manabe, T. Ito, H. Kawamura, T. Kinugasa, and Y. Sasaki, *Bull. Chem. Soc. Jpn.*, **68**, 775 (1995).
- H.-F. Eicke, M. Borkovec, and B. Das-Gupta, *J. Phys. Chem.*, **93**, 314 (1986).
- D. G. Hall, *J. Phys. Chem.*, **94**, 429 (1990).
- G. Schwarz, *J. Phys. Chem.*, **66**, 2636 (1962).
- J. Peyrelasse and C. Boned, *J. Phys. Chem.*, **89**, 370 (1985).
- T. H. Wines and P. Somasundaran, *J. Colloid Interface Sci.*, **256**, 183 (2002).
- T. Kawai, K. Hamada, N. Shindo, and K. Kon-no, *Bull. Chem. Soc. Jpn.*, **65**, 2715 (1992).
- M. J. Frisch, G. W. Trucks, H. B. Schlegel, G. E. Scuseria, M. A. Robb, J. R. Cheeseman, V. G. Zakrzewski, J. A. Montgomery, Jr., R. E. Stratmann, J. C. Burant, S. Dapprich, J. M. Millam, A. D. Daniels, K. N. Kudin, M. C. Strain, O. Farkas, J. Tomasi, V. Barone, M. Cossi, R. Cammi, B. Mennucci, C. Pomelli, C. Adamo, S. Clifford, J. Ochterski, G. A. Petersson, P. Y. Ayala, Q. Cui, K. Morokuma, N. Rega, P. Salvador, J. J. Dannenberg, D. K. Malick, A. D. Rabuck, K. Raghavachari, J. B. Foresman, J. Cioslowski, J. V. Ortiz, A. G. Baboul, B. B. Stefanov, G. Liu, A. Liashenko, P. Piskorz, I. Komaromi, R. Gomperts, R. L. Martin, D. J. Fox, T. Keith, M. A. Al-Laham, C. Y. Peng, A. Nanayakkara, M. Challacombe, P. M. W. Gill, B. Johnson, W. Chen, M. W. Wong, J. L. Andres, C. Gonzalez, M. Head-Gordon, E. S. Replogle, and J. A. Pople, "Gaussian 98, Revision A.11.4," Gaussian, Inc., Pittsburgh, PA (2002).
- C. C. J. Roothaan, *Rev. Mod. Phys.*, **23**, 69 (1951).
- R. Ditchfield, W. J. Hehre, and J. A. Pople, *J. Chem. Phys.*, **54**, 724 (1971).
- H.-F. Eicke and H. Christen, *Helv. Chim. Acta*, **61**, 2258 (1978).
- A. Goto, H. Harada, T. Fujita, Y. Miwa, H. Yoshioka, and H. Kishimoto, *Langmuir*, **9**, 86 (1993).
- X. Shen, H. Gao, and X. Wang, *Phys. Chem. Chem. Phys.*, **1**, 463 (1999).